Materials Science and Engineering A 552 (2012) 283–287

Contents lists available at SciVerse ScienceDirect

Materials Science and Engineering A

journal homepage: www.elsevier.com/locate/msea

Fluxless soldering with surface abrasion for joining metal foams

Yongxian Huang[a,*], Jing Gong[a], Shixiong Lv[a], Jinsong Leng[b], Yao Li[b]

[a] State Key Laboratory of Advanced Welding and Joining, Harbin Institute of Technology, Harbin 150001, People's Republic of China
[b] Center for Composite Materials and Structures, Harbin Institute of Technology, Harbin 150001, People's Republic of China

ARTICLE INFO

Article history:
Received 18 November 2011
Received in revised form 14 May 2012
Accepted 15 May 2012
Available online 24 May 2012

Keywords:
Aluminum foam
Surface abrasion
Soldering
Interdiffusion

ABSTRACT

Fluxless soldering with surface abrasion has been developed for joining aluminum foams. To improve the wettability of the molten filler metal on the joined surfaces, 2 methods of abrasion were used to remove the oxide film from the aluminum foams prior to soldering. The effectiveness of the abrasion was determined by microstructure observation. The mechanical properties of the joints were examined by tension and compression tests. Assisting with the mechanical abrasion, fluxless soldering using a Zn-based alloy was proven suitable for joining aluminum foams. The joints showed no visible macroscopic deformation and did not cause the foam structure to collapse, which indicates a good wetting process. The mechanical properties of the joints were similar to the parent material, and a higher compressive strength was achieved. Fluxless soldering with surface abrasion not only offers an alternative means to join aluminum foams but also lays the foundation for joining metal foams by soldering.

1. Introduction

Aluminum foam is a type of metallic foam that can offer a unique combination of several (apparently contradictory) properties that cannot be obtained in 1 conventional material (e.g., ultra-low density, high stiffness, the ability to absorb crash energy, low thermal conductivity, low magnetic permeability, and good vibration damping). More detailed information regarding aluminum foams has been presented by Banhart and co-workers [1–3]. Due to their ultra-low density combined with their excellent mechanical properties, aluminum foams have incited much interest [3–7]. In combination with new constructional principles, aluminum foams could replace conventional stamped steel parts and lead to significant weight reductions. In the aerospace industry, finding solutions to reduce the weight of planes is an intense topic of study that will mean less required fuel and lower costs. Clearly, using aluminum foams cannot only bring huge economic benefits but can also save many resources and energy if aluminum foams can successfully be applied to aircraft manufacturing [8–10].

Currently, aluminum foams can be manufactured in a variety of ways, such as solid–gas eutectic solidification, casting and powder compact melting [1]. In terms of existing techniques, it is difficult to attain large aluminum foam products and complicated structures, which is a key obstacle in expanding the real applications of aluminum foams. 1 alternative is to join aluminum foams with other foams to form an integrated structure [11], for which welding is the primary method used. However, because of the characteristics of the fusion welding process itself, the collapse of the foam structure is unavoidable [12,13]. Additionally, welding with pressure, such as ultrasonic torsion welding, pressure welding, and diffusion welding, will likely cause unacceptable deformation [14,15]. A collapsed foam structure and deformation will have significantly negative effects on the mechanical properties of aluminum foams [6,7]. These imperfections have motivated people to search for methods that will not cause the foam structure to collapse or produce macroscopic visible deformations. Several methods based on brazing and soldering have been investigated [16,17]. However, there is still much work needed to determine suitable filler metals and the proper methods to remove the oxide film on aluminum foams, which greatly impedes obtaining a reliable joint. Overall, efficient methods of joining are still in the state of testing and evaluation.

In the present work, a fluxless soldering method with surface abrasion has been developed for joining aluminum foams. Microstructure observation and thermodynamic analysis were conducted to investigate the soldering seam. The mechanical properties of the joints were examined by tension and compression tests.

2. Experimental setup

In this study, closed-cell aluminum foam produced by the blowing agent method was supplied by Southeast University of China. The chemical composition of the foam was Al–1.2 wt% Ca–1.1 wt% Ti–0.3 wt% Zn, and the mean cell size was approximately 2–3 mm. The density variation was 0.22–0.35 g/cm^3, and the porosity was approximately 90%. These foam blocks were cut to dimensions of

* Corresponding author. Fax: +86 451 86416186.
E-mail address: yxhuang@hit.edu.cn (Y. Huang).

0921-5093/$ – see front matter © 2012 Elsevier B.V. All rights reserved.
http://dx.doi.org/10.1016/j.msea.2012.05.041

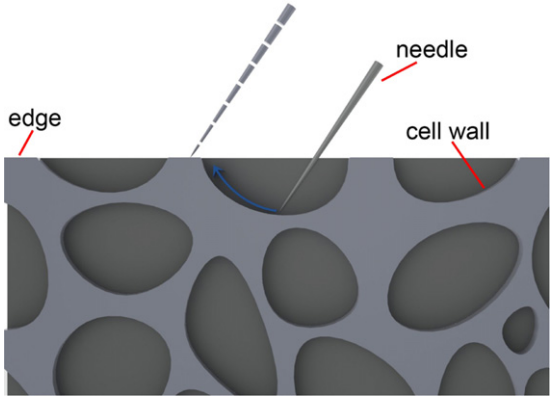

Fig. 1. Abrasion process with a needle.

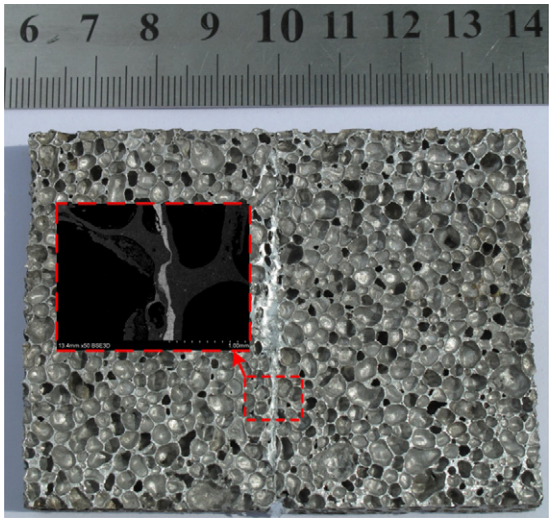

Fig. 2. Macroscopic image of a soldering joint of an aluminum foam. The inset is the enlarged interface.

80 mm × 10 mm × 25 mm by electric discharge machining (EDM), and the platelets were then rinsed in acetone. The filler metal, a Zn-based alloy, was composed of 6.2 wt% Al, 4.3 wt% Cu, 1.2 wt% Mg, 0.8 wt% Mn, 0.5 wt% Ag and balance Zn. Its melting point was in the range of 396–405 °C.

Prior to soldering, 2 methods of abrasion were used on the bonding faces, which can be summarized as follows: (1) abrasion with SiC abrasive paper, (2) abrasion with needles (by an ordinary needle that is normally used in sewing). With the abrasive paper, only the oxide film on the face was removed. For clarity, the abrasion process with the needle is shown in Fig. 1. Approximately 20% of the exposed cell walls on the bonding interfaces were abraded 5–7 times.

Manual oxygen-propane torch soldering was performed in air. The volume ratio of the oxygen and propane was 5:1. The heat treatment temperature was approximately 420 °C. When the braze alloy was melted, it was coated on the face of the aluminum foams while exposed to atmosphere. A steel stirrer with a 2 mm diameter was used to stir the molten solder metal to ensure the molten metal was homogeneous over all of the cell edges. The thickness of the soldering seams was controlled over a range from 0.2 mm to 0.5 mm. The manual oxygen-propane torch butt soldering was performed on 2 aluminum foams that underwent the same abrasion process in air, where the pressure was loaded to 2–3 kPa for 2 min. For convenience, the joints whose aluminum foams were scraped by the SiC abrasive paper are denoted 'case 1' and those treated with needles are denoted 'case 2'.

The microstructure and chemical composition of the joints were analyzed using a scanning electron microscope (SEM, HITACHI S-3500N) equipped with an energy dispersive spectrometer (EDS). The joints were sectioned across the interface zone for the microstructural characterization. Tension and compression tests were performed to examine the mechanical properties of the joints using a universal mechanic testing machine (Instron UTM, model 5569) at room temperature. For these tests, the density of the foams was not deliberately selected to avoid variations. All of the samples were cut from the same foam sheet. Specimens (80 mm × 10 mm × 10 mm) with a double-edge notch within the joints were prepared for the tension test, and specimens (20 mm × 10 mm × 20 mm) were prepared for the compression test. The depth of the notches was 3 mm, and 2 specimens from each case were used to conduct the tension test. The specimens were loaded at a constant rate of 0.5 mm/min and 2 mm/min for the tension and compression tests, respectively. The orientation of the specimens was perpendicular to the bond plane for the tension test, and the orientation of the specimens in the compression tests was in the direction normal to the bond plane. Additionally, in the compression tests, the load was removed once the strain reached 20%.

3. Results and discussion

The macroscopic overview of the soldered joints was conducted through visual observation. In both cases, no visible macroscopic deformation and foam structure collapse can be observed (the morphology of 1 representative sample is shown in Fig. 2). It is well known that the properties (particularly the mechanical properties) of aluminum foams depend significantly on their porosity and morphometric parameters [6,7]. Consequently, the original excellent properties of the aluminum foam were preserved during the soldering process. Wetting, spreading and capillary action of the molten filler metal are the key factors in forming a continuous, high-quality bonding layer in soldering. Capillary attraction provides the motivation to conduct spreading. It should be noted that wetting is a prerequisite for spreading and capillary action. Therefore, the degree of wettability is the common standard to evaluate a soldering method for joining a certain metal. The oxide film, however, has a significantly negative effect on the wettability. Almost no molten materials can wet a material covered in a dense oxide film [18,19]. No macroscopic cracks in the soldering seams can be seen in Fig. 2. The negative effect of the oxide film on the aluminum foam was avoided, and good wetting and spreading behaviors occurred during the soldering process.

A dense, uniform and continuous bonding layer was formed for the case 1 aluminum foams, as shown in Fig. 3(a) and (b). No soldering defects were detected. These observations directly confirm that a satisfactory wetting process was achieved, forming a continuous and dense bonding layer. 3 types of phases were identified according to their microstructural morphology and chemical composition. Each type of phase was marked with A, B, and C successively, as shown in Fig. 3(b). The EDS analysis revealed that the light gray and dark gray phases were Zn–Al solid solution (65.62 wt% Zn and 32.81 wt% Al) and Al–Zn solid solution (74.61 wt% Al and 22.52 wt% Zn) phases, respectively. The remaining white phases were composed of 92.76 wt% Zn and a small amount of Al (3.95 wt%). Al and Zn elements were distributed continuously throughout the cross-sectioned joint, as shown in Fig. 3(c). These facts demonstrate that the aluminum foam base metal was dissolved into the molten filler metal, and at the same time, Zn atoms diffused into the base metal. Such interdiffusion contributed to the bonding at the atomic scale

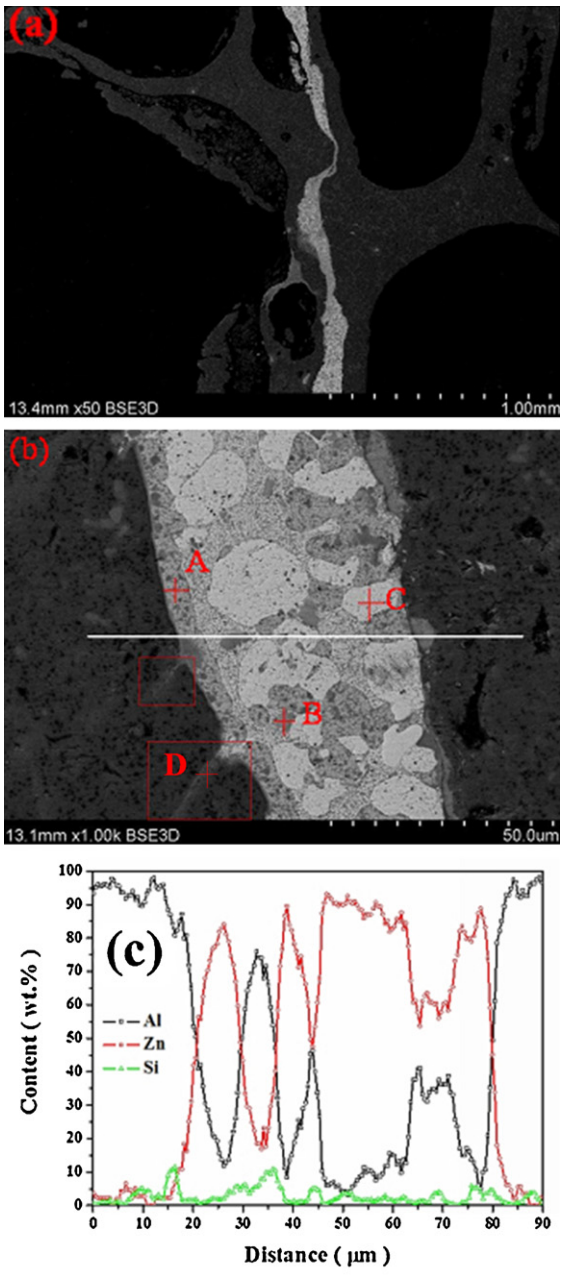

Fig. 3. SEM cross-sectional images of case 1 at different magnifications and the line-scanning analysis of the chemical composition.

and thus improved the strength of the joints. The fibrous roots, marked in Fig. 3(b), are a clear manifestation of such interdiffusion. EDS analysis was conducted on 1 typical fibrous root (marked with D), revealing that it was a Al–Zn solid solution phase (78.48 wt% Al and 20.82 wt% Zn).

Scrapes formed by the SiC abrasive paper provided more exposure for the base metal, which could be wet by the molten filler metal. More importantly, the melting point would decrease due to the change of concentration of the Al and Zn elements when the interdiffusion occurred between the aluminum foam and the soldering alloy. The process could help to break the oxide film when equilibrium was reached between the liquid phase and the solid phase, according to the polyphase equilibrium condition [20]. Considering the microstructure and element distributions, interdiffusion was formed between the aluminum foams and the Zn-based soldering alloy, and more liquid phase was formed by melting into

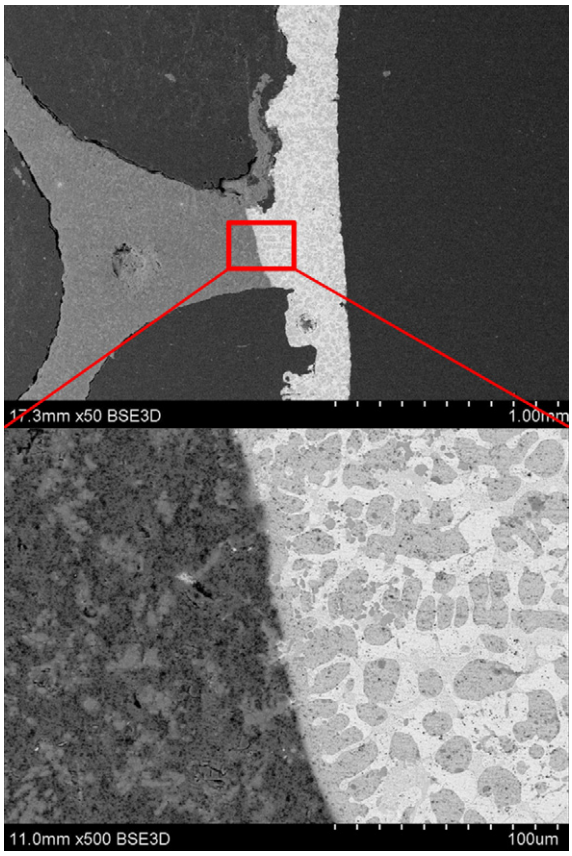

Fig. 4. SEM image of the joining interface of the aluminum foams of case 2.

the previous liquid phase. The oxide film, as a block to wetting, floated on the liquid phase due to its lower density and was then scattered during the soldering process. Additionally, the capillary attraction allowed the molten soldering alloy to spread. Consequently, the oxide film was continuously removed, and a sound joint was achieved by interdiffusion between the aluminum foam and the molten Zn-based alloy.

As shown in Fig. 4, the microstructural investigation of case 2 showed the same general features as those of case 1. However, the expected phenomenon that the molten soldering alloy would spread along the cell walls did not occur because a certain amount of the cell walls were scraped by the needle. This result can be explained by 2 main reasons. 1 reason was that the oxide film on the cell wall, which was essentially continuous, significantly impeded the spreading of the molten filler metal. The other main reason was the negative influence of the gas bubbles separated by the cell walls. As the pressure was loaded on the aluminum foam during the soldering process, gas bubbles produced a counteraction to prohibit the spreading of molten metal along the cell wall, as shown in Fig. 5. Therefore, it was almost impossible for the molten soldering alloy to spread onto the cell walls.

Fig. 5 shows the failure appearance of the tensile specimens. The fracture occurred within the aluminum foam near the soldering seam rather than at the soldering seam, even when there were notches in the seam. The soldering seam was compact in structure, and the tensile strength of the Zn–Al–Cu based alloy was much higher than that of the aluminum foams. The cell wall near the soldering seam was broken. The typical tensile strain curve is shown in Fig. 6(b). The curve shows linear elastic behavior at small strains, and the tensile strength reaches its highest value when the linear elastic behavior ends, followed by a sudden drop. The ultimate tensile strength is plotted in Fig. 6(a). Due to the non-uniformity

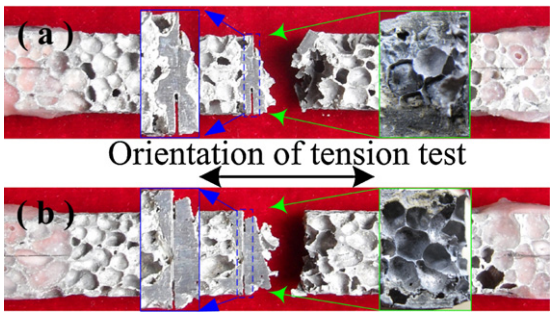

Fig. 5. The typical failure locations and appearances of the tensile specimens. (a) Case 1, (b) case 2.

of the aluminum foam, the ultimate tensile strength of the aluminum foam fluctuated between 3.75 and 5.75 MPa. Additionally, the strength of the soldering joint in cases 1 and 2 is an intermediate value. All of the failure locations on the aluminum foam were near the soldering seam, which directly indicates that the obtained soldering seams were able to withstand a greater tensile condition. Therefore, choosing aluminum foam was the decisive factor that influenced the tensile properties of the soldering structure in the present work. The tensile strength of the fluxless soldering joints was high enough to join aluminum foam.

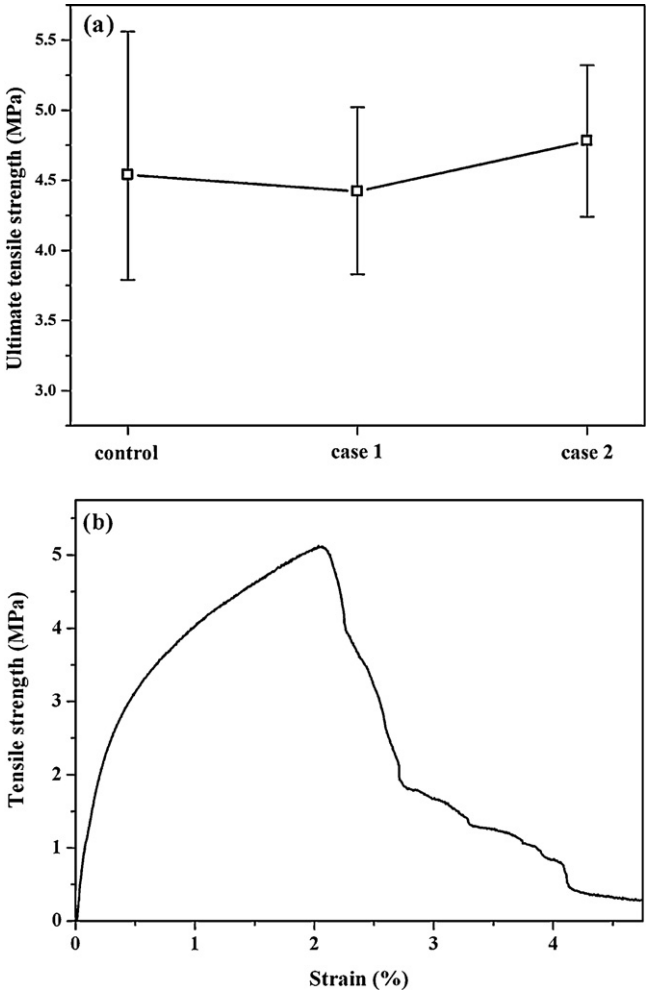

Fig. 6. The ultimate tensile strength and typical stress-strain curve. (a) The ultimate tensile strength, (b) the typical stress-strain curve.

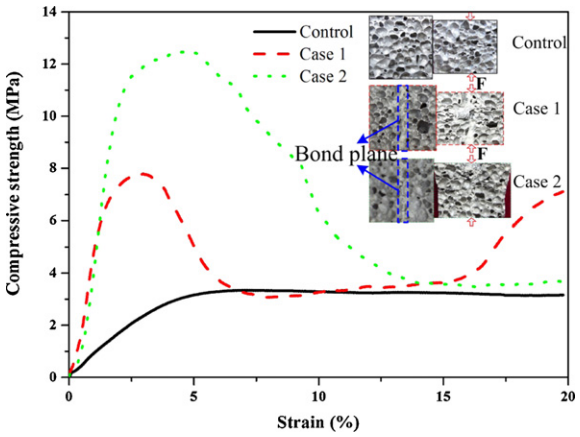

Fig. 7. Compressive stress-strain curves and appearances with a strain of 20%.

Compressive stress-strain curves for loading up to a strain of 20% are shown in Fig. 7. The compressive strength was significantly enhanced after soldering compared with that of the control aluminum foam because of the compact structure of the soldering seam, which had a much higher resistance to compression than the foam structure. When part of the soldering seam was broken, the compressive strength regressed to the value of the aluminum foam. Nevertheless, the ultimate compressive strength was still much higher than that of the control aluminum foam; the ultimate compressive strength of the aluminum foam was only 3.34 MPa. As a result, all of the joints exhibited excellent compressive properties due to the compact soldering seams.

4. Conclusion

Fluxless soldering using 2 abrasion methods was developed to join aluminum foams. There were no visible macroscopic deformations or foam structure collapses, and the original, excellent properties of the aluminum foam were preserved. In addition to similar mechanical tensile and compressive behaviors to those of the parent material, joints with a higher compressive strength were obtained. The wetting and spreading behaviors of the molten solder and the interdiffusion between the solder and aluminum foam are presented. The method of fluxless soldering with surface abrasion should be considered to join aluminum foams. Furthermore, the method is promising for joining other types of metal foam structures.

Acknowledgments

The work was jointly supported by the National Natural Science Foundation of China (no. 50904020), the Science and Technology Innovation Research Project of Harbin for Young Scholar (no. 2009RFQXG050), the Fundamental Research Funds for the Central Universities (no. HIT. NSRIF.2012007) and the China Postdoctoral Science Foundation (nos. 20090460883 and 201003419).

References

[1] J. Banhart, Prog. Mater. Sci. 46 (2001) 559–632.
[2] L.P. Lefebvre, J. Banhart, D.C. Dunand, Adv. Eng. Mater. 10 (2008) 775–787.
[3] E. Andrews, W. Sanders, L.J. Gibson, Mater. Sci. Eng. A 270 (1999) 113–124.
[4] Y. Sugimura, J. Meyer, M.Y. He, H.B. Smith, J. Grenstedt, A.G. Evans, Acta Mater. 45 (1997) 5245–5259.
[5] E. Koza, M. Leonowicz, S. Wojciechowski, F. Simancik, Mater. Lett. 58 (2003) 132–135.
[6] P.S. Liu, Mater. Sci. Eng. A 527 (2010) 7961–7966.
[7] O.B. Olurin, M. Arnold, C. Korner, R.F. Singer, Mater. Sci. Eng. A 328 (2002) 334–343.

[8] D. Schwingel, H.W. Seeliger, C. Vecchionacci, D. Alwesc, J. Dittrich, Acta Astronaut. 61 (2007) 326–330.
[9] J. Banhart, Int. J. Veh. Des. 37 (2005) 114–125.
[10] W. Hall, M. Guden, T.D. Claar, Scr. Mater. 46 (2002) 513–518.
[11] T. Bernard, H.W. Bergmann, C. Haberling, H.G. Haldenwanger, Adv. Eng. Mater. 4 (2002) 798–802.
[12] H. Haferkamp, J. Bunte, D. Herzog, A. Ostendorf, Sci. Technol. Weld. Joining 9 (2004) 65–71.
[13] U. Reisgen, S. Olschok, S. Longerich, J. Eng. Gas Turbines Power 132 (2010) 054502-1–054502-5.
[14] C. Born, H. Kuckert, G. Wagner, D. Eifler, Adv. Eng. Mater. 11 (2003) 779–786.
[15] K. Kitazono, A. Kitajima, E. Sato, J. Matsushita, K. Kuribayashi, Mater. Sci. Eng. A 327 (2002) 128–132.
[16] H. Wang, Y.S. He, M.X. Chu, D.P. He, Acta Metall. Sinica 45 (2009) 723–728.
[17] H. Wang, D.P. He, M.X. Chu, Y.S. He, Trans. Chin. Weld. Inst. 29 (2008) 1–4.
[18] T. Jarvis, W. Voice, R. Goodall, Mater. Sci. Eng. A 528 (2011) 2592–2601.
[19] G.H. Findenegg, S. Herminghaus, Curr. Opin. Colloid Interface Sci. 2 (1997) 301–307.
[20] J.L. Murray, J. Phase Equilib. 4 (1983) 55–73.